Oecologia (2024) 205:307–322
https://doi.org/10.1007/s00442-024-05572-5

ORIGINAL RESEARCH

Invertebrate sounds from photic to mesophotic coral reefs reveal vertical stratification and diel diversity

Xavier Raick[1] · Éric Parmentier[1] · Cédric Gervaise[2] · David Lecchini[3,4] · Under The Pole Consortium · Gonzalo Pérez-Rosales[3] · Héloïse Rouzé[3,5] · Frédéric Bertucci[1,3] · Lucia Di Iorio[6]

Received: 14 November 2022 / Accepted: 27 May 2024 / Published online: 3 June 2024

Abstract

Although mesophotic coral ecosystems account for approximately 80% of coral reefs, they remain largely unexplored due to their challenging accessibility. The acoustic richness within reefs has led scientists to consider passive acoustic monitoring as a reliable method for studying both altiphotic and mesophotic coral reefs. We investigated the relationship between benthic invertebrate sounds (1.5–22.5 kHz), depth, and benthic cover composition, key ecological factors that determine differences between altiphotic and mesophotic reefs. Diel patterns of snaps and peak frequencies were also explored at different depths to assess variations in biorhythms. Acoustic recorders were deployed at 20 m, 60 m, and 120 m depths across six islands in French Polynesia. The results indicated that depth is the primary driver of differences in broadband transient sound (BTS) soundscapes, with sound intensity decreasing as depth increases. At 20–60 m, sounds were louder at night. At 120 m depth, benthic activity rhythms exhibited low or highly variable levels of diel variation, likely a consequence of reduced solar irradiation. On three islands, a peculiar peak in the number of BTS was observed every day between 7 and 9 PM at 120 m, suggesting the presence of cyclic activities of a specific species. Our results support the existence of different invertebrate communities or distinct behaviors, particularly in deep mesophotic reefs. Overall, this study adds to the growing evidence supporting the use of passive acoustic monitoring to describe and understand ecological patterns in mesophotic reefs.

Keywords Broadband transient sounds · Snapping shrimps · Benthic invertebrate sounds · French Polynesia · Mesophotic coral ecosystems

Introduction

Most marine habitats are filled with biological sounds, which can be either communication signals and/or sounds emitted as by-products of animal activities such as feeding or movement (Ladich 2015). The composition of sounds within a given habitat depends on the diversity of species present, their behavior, and activities, which are influenced by ecological and environmental factors (Pijanowski et al. 2011; Desjonquères et al. 2018; Raick et al. 2023). The study of animal sounds within an ecological framework is the core objective of ecoacoustics (Sueur and Farina 2015). It represents an innovative and effective monitoring technique for non-invasively acquiring information on biodiversity, behaviors, and biorhythms, irrespective of water turbidity, temperature, or depth (Gibb et al. 2019; Bolgan et al. 2020; Favaro et al. 2021; Di Iorio et al. 2021). Soundscapes, encompassing all sounds emanating from an ecosystem, also provide information on cryptic species and their activities

Communicated by Joel Trexler.

The members of Under The Pole Consortium is listed in acknowledgments section.

✉ Xavier Raick
xavier.raick@uliege.be

1 Laboratory of Functional and Evolutionary Morphology, Freshwater and Oceanic Science Unit of Research, University of Liège, Liège, Belgium

2 Chorus Institute, Grenoble, France

3 PSL University, EPHE-UPVD-CNRS, USR, CRIOBE, 3278 Moorea, French Polynesia

4 Laboratoire d'Excellence "CORAIL", Perpignan, France

5 Marine Laboratory, University of Guam, Mangilao, GU, USA

6 University of Perpignan Via Domitia, CNRS, CEFREM, UMR 5110, Perpignan, France

24 h a day, making them suitable for assessing cryptic biodiversity. Recording these sounds and their variability is therefore promising, particularly for studying less accessible ecosystems such as mesophotic coral ecosystems (MCEs) (Lin et al. 2019; Raick et al. 2023a, b).

Mesophotic coral ecosystems, extending roughly from depths of 30 to 150 m (Hinderstein et al. 2010; Pyle et al. 2016; Baldwin et al. 2018), constitute approximately 80% of tropical coral reefs (Loya et al. 2019). Despite their significant contribution to reef ecosystems, little is known about their ecology and functioning (Pyle et al. 2016; Raick et al. 2023), primarily due to the challenges in accessing and collecting scientific data at such depths. The limited studies conducted in mesophotic reefs have documented high spatial heterogeneity and structural complexity, providing shelter to a myriad of species (Lesser et al. 2009; Weinstein et al. 2015; Pyle and Copus 2019). Knowledge of mesophotic soundscapes, including the diversity of biological sounds and their variability, remains very limited. It is largely unknown whether acoustic composition and patterns are specific to MCEs, to what extent they differ from altiphotic reefs, and whether lower light conditions influence biorhythms. Most studies on coral reef sounds have been conducted in the altiphotic zone (Bertucci et al. 2020; Minier et al. 2023a, b). The major sources of biological sounds in these altiphotic coral reefs are benthic invertebrates, fish, and cetaceans. Fish and whales vocalize mainly in the low-frequency band (below 2 kHz) while dolphins and most benthic invertebrates can emit broadband transient sounds (BTS), generally at higher frequencies (> 2 kHz) (Mooney et al. 2020). To provide ecologically relevant information about specific environments, the biogenic sound composition and/or acoustic patterns of a soundscape should be linked to habitat features.

Depth is an important driver influencing the composition of animal communities (Kahng and Kelley 2007; Milligan et al. 2016). The depth-dependent composition and abundance of fish sounds has been documented in coral and temperate red-algae coralligenous reefs, likely reflecting the vertical stratification observed in fish assemblages (Di Iorio et al. 2021; Raick et al. 2023). Furthermore, the acoustic community composition of fish is strongly linked to benthic cover composition (e.g., the percentage of living fixed organisms) in temperate red-algae coralligenous reefs, as well as altiphotic and mesophotic coral reefs (Bertucci et al. 2016; Di Iorio et al. 2021; Raick et al. 2023). This indicates that acoustic cues can be associated with habitat-specific features. Depth-dependent distributions of benthic assemblages have been described for various coral reefs based on visual data (Goreau and Goreau 1973; Liddell and Ohlhorst 1988; Kahng and Kelley 2007; Lesser et al. 2019; Pérez-Rosales et al. 2022a). Additionally, the three-dimensional structure of coral reefs and the presence of specific organisms such as sponges or octocorals provides shelter to a variety of often invisible invertebrate species, known to significantly contribute to the high biodiversity of coral reefs (Díaz and Rützler 2001; Chin et al. 2020). Acoustic footprints emitted by these sheltered invertebrate species reflect the activities of animal communities and may serve as proxies of biodiversity and density of benthic organisms (Kennedy et al. 2010). Most sounds produced by benthic invertebrates are broadband transient sounds (BTS) extending over tens of kilohertz, dominating coastal soundscapes day and night (UCDWR 1946; Everest et al. 1948). These sounds can be emitted by numerous species from different taxonomic groups, such as sea urchins (Radford et al. 2008; Coquereau et al. 2016), bivalves (Di Iorio et al. 2012) or numerous crustaceans such as hermit crabs (Freeman et al. 2014), crabs, stomatopods, palaemonid shrimps (Johnson et al. 1947), and snapping shrimps, specifically species from *Alpheus* and *Synalpheus* genera (Alpheidae) (Johnson 1944; Johnson et al. 1947; Au and Banks 1998; Lillis and Mooney 2018). Despite documented decreases in snapping shrimp sounds below a depth of 55 m, which are among the most prevalent sounds in coral reefs (Johnson et al. 1947; Lammers et al. 2008; Piercy et al. 2014), our understanding of depth-related differences in BTS is limited. Furthermore, there is a dearth of studies exploring the composition and contribution of BTS to soundscapes, as well as their correlation with benthic cover in mesophotic reefs.

Sounds produced by benthic invertebrates can serve as indicators of different habitats (Radford et al. 2010, 2014). Moreover, BTS, particularly those emitted by snapping shrimps, respond to environmental changes such as temperature or pH (Watanabe et al. 2002; Rossi et al. 2016; Lillis and Mooney 2018) and exhibit distinct biorhythms. In fact, in many altiphotic reefs, BTS display diel variations (Everest et al. 1948; Lillis and Mooney 2016, 2018; Raick et al. 2021), with peaks typically observed around sunrise and/or sunset (Johnson et al. 1947; Lammers et al. 2008; Raick et al. 2021). Different diel cycles can co-occur at a specific site (Lammers et al. 2008; Lillis and Mooney 2016) and are known to depend on the peak frequency of BTS, potentially indicating differences in underlying communities (Raick et al. 2021).

In this study, we investigated the relationship between benthic invertebrate sounds, depth, and benthic cover composition, key ecological factors determining differences between altiphotic and mesophotic coral reefs. Our aim was to establish whether specific BTS are found in MCEs, and whether they are possibly related to the community compositions of benthic invertebrates. Additionally, we explored the diel cycles of BTS at different depths to assess whether different light regimes affect biorhythms. Three predictions were tested: (1) altiphotic and mesophotic reefs are characterized by distinct BTS that may contribute biodiversity

differences; (2) BTS show a strong relationship to benthic cover composition, suggesting the presence of specific BTS in MCEs; (3) depth affects diel patterns of BTS, suggesting an influence on biorhythms. To test these three predictions, we used a unique dataset collected from six islands in French Polynesia, a group of islands that extends over 5 million km^2 in the South Pacific Ocean (Rancher and Rougerie 1994; Rougerie et al. 1997), at three different depths (20 m, 60 m, and 120 m) coupling passive acoustic recordings with benthic sessile cover inventories.

Materials and methods

Data collection

Data sampling was conducted between March 2018 and April 2019 on 6 islands in French Polynesia: Bora Bora, Moorea (both in the Society Archipelago), Teauaone Islet near Mangareva (Gambier Archipelago), Rangiroa, Raroia, and Tikehau (all 3 in the Tuamotu Archipelago) (Fig. 1; Table 1). The first three islands are high volcanic islands, while the last three are atolls. At each island, 3 different depths were studied concurrently on the external slope, 1 in the altiphotic reef (20 m) and 2 in the mesophotic reef (60–120 m). At Mangareva, only the 2 shallower depths were studied due to an issue with the recorder.

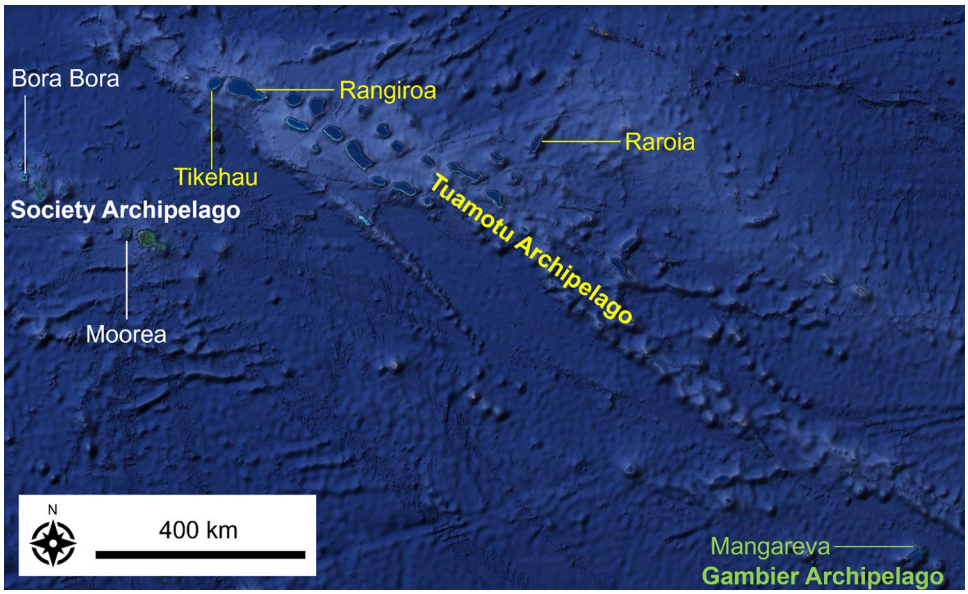

Fig. 1 Map of the central part of French Polynesia: Society Archipelago (in white), Tuamotu Archipelago (in yellow), and Gambier Archipelago (in green) with the six studied islands highlighted

Table 1 Localization (archipelago, type of island, latitude, longitude) and period of sampling (year, month, and day) for each island (N = 6)

Island	Type	Lat (S)	Long (W)	Year	Month	Day
Tuamotu Archipelago						
Rangiroa	Atoll	14.980°	147.613°	2018	Oct—Nov	30th–2nd
Raroia	Atoll	16.023°	142.463°	2018	March	2nd–5th
Tikehau	Atoll (Raised atoll)	15.017°	148.287°	2018	October	15th–18th
Society Archipelago						
Bora Bora	High island (Almost atoll)	17.477°	149.851°	2018	September	21st–24th
Moorea	High Island	16.437°	151.754°	2018	September	4th–7th
Gambier Archipelago						
Mangareva (Teauaone)	High Island	23.001°	134.960°	2019	April	16th–19th

For all the islands, three depths were sampled: 20 m, 60 m, and 120 m except at Mangareva where only the two shallower depths were studied

Tripod structures, each equipped with 4 kg of ballast and measuring 60 cm, were deployed on the sea bottom of the barrier reef at depths of 20 m, 60 m, and 120 m on each island. On the vertical pole of each tripod, an acoustic recorder SNAP / HTI96 hydrophone (Loggerhead Instruments, Sarasota, FL, USA) was attached. The recorder operated for 62 h (1 min on / 9 min off, flat frequency response between 2 and 30,000 Hz, sampling frequency: 44.1 kHz, resolution: 16-bit, gain: + 2.05 dB, sensitivity: − 170.5 to − 169.7 dB re 1 V for a sound pressure of 1 µPa). The recorded files were categorized into four temporal periods: day (07 AM – 04:59 PM, n = 2 per depth and island), sunset (05 PM – 06:59 PM, n = 3), night (07 PM – 04:59 AM, n = 3), and sunrise (05 AM – 06:59 AM, n = 3).

To assess benthic cover, we used photo-quadrats from Raick et al. (2023). For each island, photo-quadrats were realized during each deployment and employed to characterize the benthic sessile cover. At each depth, ten non-superimposed 0.75 × 0.75 m photo-quadrats were taken along four 10 m-long lines leaving a constant of 25 cm between quadrats following the methodology described by Pérez-Rosales et al. (2022b). Subsequently, 90 pictures out of 120 (30 pictures out of 40 per depth) were randomly selected. The benthic cover was categorized into 16 classes: (1) sand, (2) dead coral, (3) rubble, (4) consolidated substrate, (5) scleractinian, (6) black coral and gorgonians, (7) Anthoathecata, (8) other hydroids, (9) encrusting sponges, (10) non encrusting sponges, (11) turf, (12) calcifying algae, (13) fleshy algae, (14) macroalgae including *Halimeda* algae, (15) encrusting algae and (16) other sessile invertebrates (Raick et al. 2023). The photo-quadrats were analyzed using Photoquad 1.4 software (University of the Aegean, Mytilene, Greece), following the methodology developed by Pérez-Rosales et al. (2022b). Percentages of each category per quadrat were averaged to obtain mean values for each depth and island. These data were then used for the redundancy analysis (see 'Link between BTS and benthic cover' section).

Acoustic analysis

Spectral density

To assess patterns of mass phenomena of BTS production, we calculated Power Spectral Densities (PSD) using custom-made Matlab routines (version R2014b) with parameters set to FFT = 256, Kaiser window, and overlap = 50% (MathWorks, Natick, MA, USA). Median ($Q_{0.50}$) spectra were generated for each depth (20 m, 60 m, and 120 m), each period (day, night, sunrise, and sunset) and each replicate (Bora Bora, Mangareva, Moorea, Rangiroa, Raroia, and Tikehau). Two features were measured on each spectrum: the highest power spectral density value ($\mathbf{PSD_{Fpeak}}$, in dB re 1 µPa^2 Hz^{-1}) and the corresponding frequency (**γFpeak**, in kHz, Fig. 2), representing the frequency at which the power spectral density is maximal (Jézéquel et al. 2018). To compare PSD values corresponding to the same frequency at different depths, the difference between the peak frequency at 20 m was compared to the corresponding frequency at 60–120 m and referred to as $\mathbf{\Delta_{20m}}$ (in dB re 1 µPa^2 Hz^{-1}) (Fig. 2).

Acoustic features of single BTS

In addition to the acoustic characterization of the mass phenomena, acoustic features were extracted from each BTS, selected using an automatic BTS detector (Gervaise et al. 2019) applied to the audio recordings through a custom-made Matlab routine (version R2014b, MathWorks, Natick, MA, USA). The signal was filtered, and its energy was calculated. Subsequently, the ambient noise level (ANL) was estimated, and based on this ANL and a target false alarm

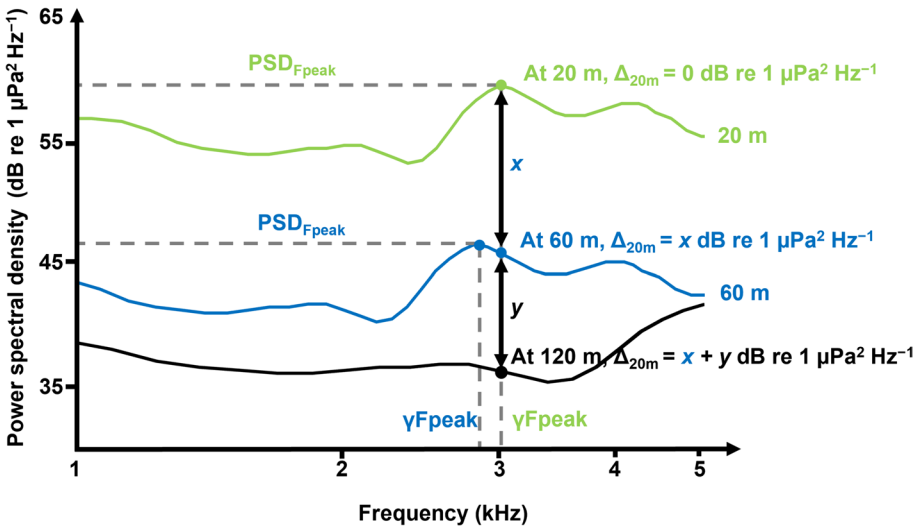

Fig. 2 Graphical representation of the parameters measured on Power Spectral Densities (PSD) graphs. Green line: median at 20 m, blue line: median at 60 m, and black line: median at 120 m. The horizontal axis is frequency in logarithmic scale. PSD_{Fpeak} highest power spectral density value, γFpeak corresponding frequency, and Δ20m difference between the peak frequency at 20 m compared to the corresponding frequency at 60 or 120 m

probability, a detection threshold was computed using the energy of the signal (Gervaise et al. 2019). If the local energy exceeded the detection threshold, a BTS was identified (Gervaise et al. 2019). To avoid inclusion of sounds other than those produced by benthic invertebrates, the recordings were first visually and aurally inspected with RavenPro Sound Analysis Software 1.5 (Cornell Lab of Ornithology, USA) for frequencies between 1.5 and 22.05 kHz, with the aim of removing recordings containing echolocation clicks of odontocetes and masking anthropogenic noise. For each 1 min file, 3 features were computed: (1) the number of detected BTS per second (**NoBTS**, in BTS s^{-1}) with a minimum signal-to-noise ratio of 10 dB, (2) their peak frequency (**BTS Fpeak**, in kHz) and (3) the broadband-peak-to-peak Sound Pressure Level (SPL_{pp}) (**BTS SPL_{pp}**, in dB re 1 µPa) (Raick et al. 2021). γFpeak reflects mass-phenomena differences, while BTS Fpeak provides an indication on the diversity of individual BTS.

Statistical analysis

Depth variability of BTS

To evaluate the depth variability of BTS, the power spectra of each depth (20 m, 60 m, and 120 m) were initially compared visually. Five linear mixed-effect models (function *lme*, package *nlme*) were then employed: 1 for each acoustic feature derived from the power spectra (PSD_{Fpeak} and γFpeak), as well as individual BTS features (NoBTS, BTS Fpeak, and BTS SPL_{pp}). Depth (20 m, 60 m, and 120 m) and temporal periods (sunset, night, sunrise, and day) were designated as fixed factors, nested within the season (as a random effect). For spectral features (PSD_{Fpeak}, γFpeak, and Δ_{20}), 187 datapoints were used (11 temporal replicates per island and per depth). For the acoustic features of individual BTS (NoBTS, BTS Fpeak and BTS SPL_{pp}), the dataset comprised between 5465 and 5752 data points (1 value per file was used, i.e., 36 for sunset and sunrise periods, 120 for the day, and 180 for the night). The variation in data points is due to some files lacking sufficient BTS to determine BTS SPL_{pp} and BTS Fpeak. The significance level was set to $\alpha = 0.05$. Subsequent between-depth comparisons were conducted with Tukey tests (function *glht*, package *multcomp*, with Bonferroni correction). Bonferroni corrections were applied to counteract the multiple comparisons problem and avoid Type I errors. Following this, acoustic features were compared among islands to investigate spatial variability. Non-parametric Kruskal–Wallis tests (with Dunn's test as *post-hoc* analysis, employing a Benjamini–Hochberg correction on *P*-values) were separately conducted for each island to compare the 3 depths (20 m, 60 m, and 120 m). In Mangareva, a Mann–Whitney-U test was used instead to compare the two sampled depths (20 and 60 m). These tests were chosen due to non-compliance with normality and/or homoscedasticity of variances. All statistical analyseswere performed using R software version 3.6.1. (R Core Team, 2019).

Link between BTS and benthic cover

A redundancy analysis (RDA) was performed to examine the relationship between benthic sessile cover features and acoustic characteristics (library *vegan*, function *rda;* https://cran.r-project.org/web/packages/vegan/vegan.pdf*) (Oksanen et al. 2012). RDA, commonly applied in ecology (Kopp et al. 2012), employs multiple linear regressions to assess the variation between independent features (explanatory variables) and dependent features (response variables). It captures the primary patterns of species variation and presents correlation coefficients between each independent and dependent feature (ter Braak 1994; Ramette 2007). It can be considered as an extension of principal component analysis (PCA), in which components are constrained to linear combinations of environmental features (Rao 1964). Acoustic features (*PSD_{Fpeak}*, γFpeak, Δ_{20m}, NoBTS, BTS Fpeak, BTS SPL_{pp}) were standardized (to 0 mean and unit variance) and used as response variables, while cover features were used as explanatory variables. To aid in interpretating *site constraints*, Spearman correlations, with associated *P*-values adjusted by Holm's method, were calculated between *site constraints* and acoustic features.

Diel variability of BTS

Spectrograms and PSD graphs between 1 and 20 kHz were generated with custom-made Matlab routines (version R2014b) for the temporal periods (day, night, sunrise, and sunset). These were visually compared to evaluate the diel variability of BTS. In addition, time series analyses (with 1 data point per 10 min) were performed on the 62 h of recordings for NoBTS, BTS Fpeak and BTS SPL_{pp} and the results were graphically presented.

To assess the influence of the different acoustic features, a linear mixed-effect model (function *lme*, package *nlme*) was performed for each studied depth (20 m, 60 m, and 120 m) and acoustic feature (PSD_{Fpeak}, γFpeak, NoBTS, BTS Fpeak, and BTS SPL_{pp}). Temporal period (sunset, night, sunrise, or day) was used as fixed-effects factor, nested within the season (considered as as random effect). For the spectral features (PSD_{Fpeak}, γFpeak and Δ_{20}), we used between 55 (120 m) and 66 data points (20 and 60 m). In the case of acoustic features of BTS (NoBTS, BTS Fpeak and BTS SPL_{pp}), the dataset comprised between 1341 and 2152 data points. The significance threshold was set at $\alpha = 0.05$. Diagnostic plots were employed to verify model assumptions. Multiple comparisons (Tukey tests) between depths

were conducted with Bonferroni corrections (function *glht*, package *multcomp*). Additionally, acoustic features were compared among islands to explore inter-island variability. Mann–Whitney U tests and Kruskal–Wallis tests (followed by Dunn's test as *post-hoc* with a Benjamini–Hochberg correction on *P*-values) were employed to compare temporal periods at each depth.

Results

Depth variability

General pattern

The spectrograms and PSD graphs revealed that the soundscape at the frequency range [1.5,22 kHz] was predominantly characterized by broadband transient sounds (BTS) produced by benthic invertebrates (Fig. SP1). When considering all depths and all islands, the highest values of power spectral density (PSD_{Fpeak}) were found between 3 and 10 kHz, displaying variations in both the number and intensity of spectral peaks. As depicted in Fig. 3, at a depth of 20 m, γF_{peak} predominantly ranged between 5 and 6 kHz, aligning with the characteristic spectral increase associated with snapping shrimp (Everest et al. 1948; Ferguson and Cleary 2001). The variability in γF_{peak} was more pronounced at 60 and 120 m depths. At 60 m, γF_{peak} seemed to fluctuate between 4 and 10.5 kHz, depending on the island, while at 120 m, γF_{peak} exhibited variations from 2.9 to 6.4 kHz (Fig. 3). BTS beyond 2–4 kHz consistently surpassed the average Wenz ambient noise level, i.e., the ambient noise level in the presence of a 6-knot wind (Raick et al. 2021).

The spectral acoustic features of the mass phenomena of BTS and those extracted from individual BTS events identified using the automatic detector were significantly influenced by depth (Fig. 3; Table 2). The highest power spectral density value (PSD_{Fpeak}) decreased with increasing depth (71.7, 63.7 and 57.8 dB re 1 $\mu Pa^2\ Hz^{-1}$ at 20, 60–120 m, respectively). The difference was statistically significant between 20 and 60 m but not between 60 and 120 m (Table 2). The frequency corresponding to the highest power spectral density value (γF_{peak}) also varied with depth; it was consistent between 20 and 60 m but approximately 2 kHz lower between 60 and 120 m. Both BTS SPL_{pp} and the number of BTS decreased with increasing depth, while the opposite trend was observed for BTS Fpeak (Table 2) (Fig. 4). γFpeak and BTS Fpeak were equivalent at 20 m (5.50 kHz vs. 5.37 kHz) and at 60 m (5.88 kHz vs. 5.98 kHz) but showed a substantial difference at 120 m (3.89 kHz vs. 8.22 kHz). This discrepancy between γFpeak and BTS Fpeak is likely attributed to the low number of detections at 120 m.

Differences among islands The depth effect on acoustic features was not consistent across all islands. Moorea and Bora Bora exhibited highly contrasting patterns. In Moorea, similar values for PSD_{Fpeak}, Δ20, and BTS SPL_{pp} were observed between 60 and 20 m, whereas in Bora Bora, the similarity was between 60 and 120 m (Fig. 3., Table SP1). These differences may be attributed to three factors: slope, temperature (Fig. SP2), and/or substrate composition.

The pattern of a decreasing number of BTS with increasing depth was not consistently observed across all islands (Table 1). In Bora Bora and Raroia, the number of BTS was 1.3–1.5 times higher at 60 m than at 20 m depth. At 120 m, a high number of BTS was observed for Raroia and Tikehau, while a lower number of BTS was recorded for Bora Bora, Moorea, and Rangiroa.

Link between BTS and benthic cover

The redundancy analysis (RDA) indicated that acoustic features were primarily influenced by depth. Inspection of the RDA plot enables the association of benthic cover features, sites, and acoustic features (Fig. 5, Table SP3). Positive RDA1 values were predominantly explained by non-encrusting sponges, sand, hydroids, other sessile invertebrates, "black coral and gorgonians" (RDA1 scores: 0.70, 0.67, 0.67, 0.62, and 0.58, respectively). BTS peak frequency appears to be associated with these features as well as with greater depths (Fig. 5). In contrast, negative RDA1 values were primarily explained by macroalgae, scleractinians, and dead coral (−0.64,− 0.55, and−0.50, respectively). PSD_{Fpeak}, Δ20, and BTS SPL_{pp} features were grouped together and significantly negatively correlated with RDA 1 ($\rho = -0.95, -0.92$ and -0.96, all $P < 0.0001$). In addition, the number of BTS tended to be associated with shallow reefs (Fig. 5) (Table 3). This reflects the lower benthic acoustic activity observed in deep mesophotic reefs. RDA2 to RDA6 did not correlate with any acoustic features.

Diel variability

General pattern

Though diel cycles were evident (Fig. SP1), variation in diel patterns was observed for most acoustic features (Fig SP1). PSD_{Fpeak} was generally higher at night than during the day, except at a depth of 120 m, where the patterns varied among islands (Table 4, Fig. 6A, SP2, SP3 and SP4). Altiphotic reefs exhibited the highest PSD values, followed by mesophotic reefs at depths of 60– 120 m. BTS Fpeak displayed consistent diel patterns at 20–60 m depth, but with higher variability at 120 m depth (Fig. 6) At 20 m, BTS Fpeak differed at sunset compared to daytime and night. However, no significant differences were found between night and day

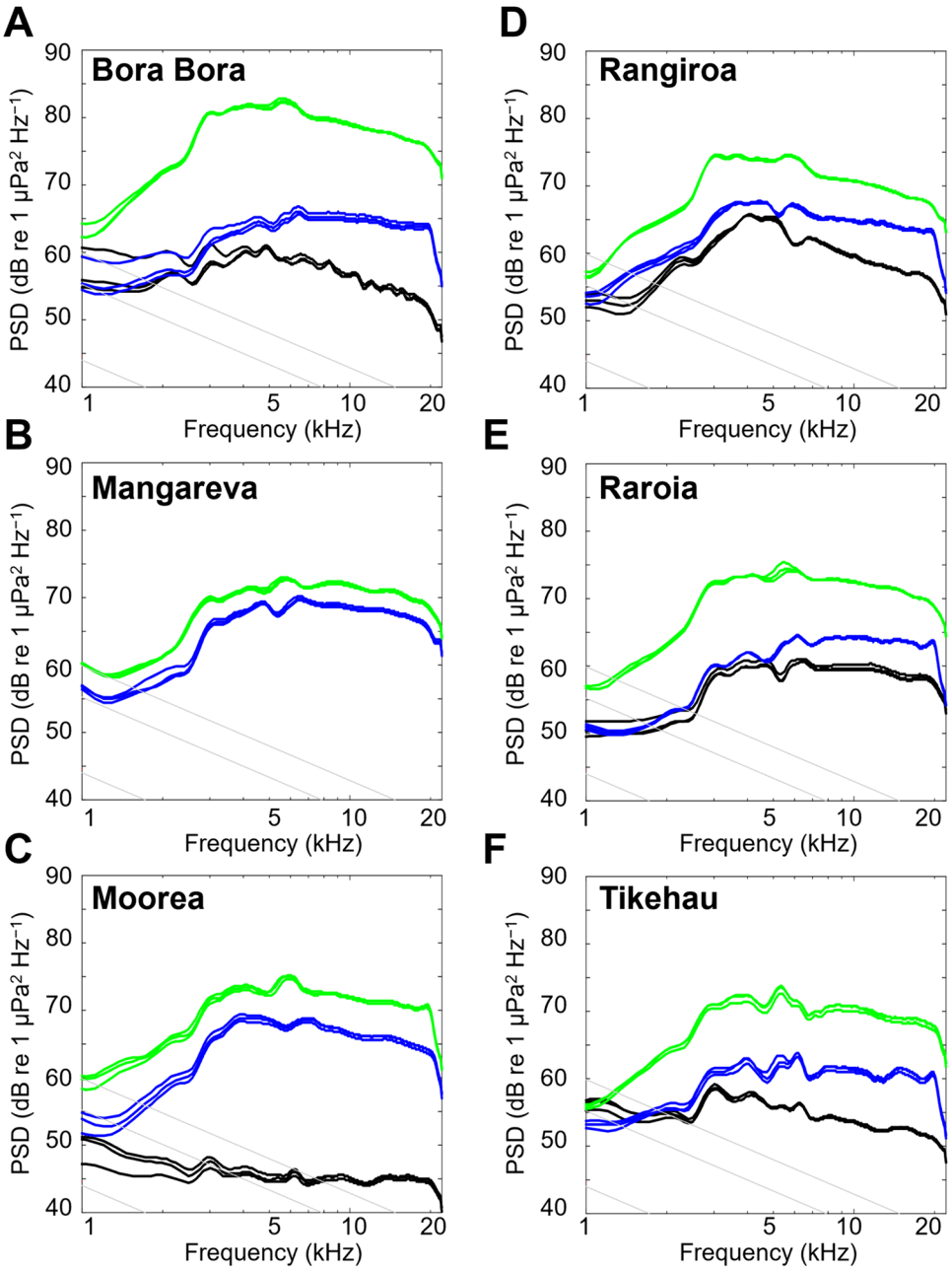

Fig. 3 Median Power Spectral Density (PSD) during the night per island. **A** Bora Bora, **B** Mangareva, **C** Moorea, **D** Rangiroa, **E** Raroia and **F** Tikehau. In green: 20 m, in blue: 60 m, and in black: 120 m. Each line is a replicate (night n°1, n°2 and n°3). In grey, Wenz ambient noise level curves for wind speeds 0 kn, 6 kn and 12 kn (from bottom to top). The horizontal axis is frequency in logarithmic scale

(Table 4). In contrast, in mesophotic reefs (60–120 m) diurnal and nocturnal BTS Fpeak differed significantly (Table 4), indicating potential activity switches in the communities of the emitting species. Finally, the number of BTS and the BTS SPL_{pp} presented diel variations at all depths, but distinct patterns were observed. Particularly at 120 m depth, diel variability was highly variable among islands (Table 4; Fig. 6). At 120 m depth, the number of BTS did not show a general diel pattern, as indicated by the highly variable time series, suggesting no generalizable diel rhythms in the activity of benthic invertebrates. (Fig. 6C, Table SP8).

There was an increase in the number of BTS around 7 PM that lasted for two hours at the three islands of Bora Bora (6:50–7 to 8:30–8:50 PM), Moorea (6:30 to 7:40–7:50 PM), and Tikehau (6:30–6:40 to 8:00–9 PM). Indeed, the number of BTS was 37.7% to 97.7% higher during this period compared to the 2 h before and after (Table SP15). The peak frequency of the BTS during this 2 h increase was around 5.4 kHz, significantly different from the peak frequency of the BTS the 2 h before and after (Table SP15). This suggests an activity onset of a specific species peaking between 7 and 9 PM. When examining the variation in PSD graphs at a depth of 120 m in detail, peaks of 10–20 min in duration are observed. For example, at Bora Bora, an increase of 5 dB re 1 $\mu Pa^2\,Hz^{-1}$ between 7.3 and 8 kHz is observed at 6:40 PM – 6:50 PM (Fig. 7), while a less intense but longer

Table 2 Linear mixed-effect model results with multiple comparisons (Tukey tests) to access depth variability

		Z value	*P*
PSD_{Fpeak} (F = 212.16, *P* < .0001) N = 187	20 vs. 60	− 4.64	**< .0001**
	20 vs. 120	− 6.06	**< .0001**
	60 vs. 120	− 1.64	0.30
γFpeak (F = 48.21, *P* < .0001) N = 187	20 vs. 60	− 0.18	≈ 1.00
	20 vs. 120	− 4.30	**< .0001**
	60 vs. 120	− 4.13	**0.00011**
Δ_{20} (F = 306.15, *P* < .0001) N = 187	20 vs. 60	− 5.62	**< .0001**
	20 vs. 120	− 8.90	**< .0001**
	60 vs. 120	− 3.55	**0.0012**
BTS SPL_{pp} (F = 9342.4, *P* < .0001) N = 5732	20 vs. 60	− 38.73	**< .0001**
	20 vs. 120	− 64.71	**< .0001**
	60 vs. 120	− 27.39	**< .0001**
NoBTS (F = 1445.14, *P* < .0001) N = 5752	20 vs. 60	− 6.72	**< .0001**
	20 vs. 120	− 37.38	**< .0001**
	60 vs. 120	− 30.23	**< .0001**
BTS Fpeak (F = 640.171, *P* < .0001) N = 5465	20 vs. 60	6.66	**< .0001**
	20 vs. 120	23.41	**< .0001**
	60 vs. 120	17.02	**< .0001**

P-values are adjusted with Bonferroni corrections. **PSD_{Fpeak}** = highest power spectral density value, **γFpeak** = corresponding frequency, **Δ20m** = difference between the peak frequency at 20 m compared to the corresponding frequency at 60 or 120 m, **BTS SPL_{pp}** = peak-to-peak sound pressure level of the broadband transient sounds, **NoBTS** = number of broadband transient sounds, and **BTS Fpeak** = peak frequency of the broadband transient sounds. α = 0.05. N = 187 for the three first features and 5465 to 5752 for the three last ones

increase was observed from 7:10 PM to 7:50 PM between 4.6 and 5 kHz (Fig. 7). These observations likely represent activities of species specific to the deep part of mesophotic reefs (120 m).

Differences among islands

Overall, PSD_{Fpeak} diel patterns at 20–60 m depth were similar across islands. At 120 m, some islands (e.g., Rangiroa and Raroia) exhibited PSD_{Fpeak} patterns resembling those at 20 m while others (e.g., Moorea) displayed opposite patterns (not statistically supported) (Fig. 6A, Fig. SP3, Table SP4). γF_{peak} remained constant throughout the day at all depths on some islands, whereas diel cycles were observed in certain mesophotic reefs, with a higher γF_{peak} during the night or day, suggesting that acoustic mass phenomena vary, or not, depending on the site/island (Fig. SP4 and SP5). The diel variation of the number of BTS at 20–60 m was relatively consistent across islands, with generally higher values during the day than at night, (but see Bora Bora and Raroia, Fig. 6C, Table SP6 and SP7).

Discussion

Depth variability

The underwater acoustic survey conducted at three different depths across six islands in French Polynesia revealed significant differences in the sounds emitted by benthic invertebrates. Despite the brief sampling period, it was evident that depth was the primary factor influencing benthic transient sounds, as indicated by depth-related differences in almost all acoustic parameters.

The acoustic features of benthic invertebrate sounds were found to be correlated with the sessile benthic cover structure. At a depth of 120 m, marked differences in peak frequencies were observed compared to the BTS recorded at 60–20 m depth, likely reflecting distinct benthic communities. Thus, the sounds emitted by benthic

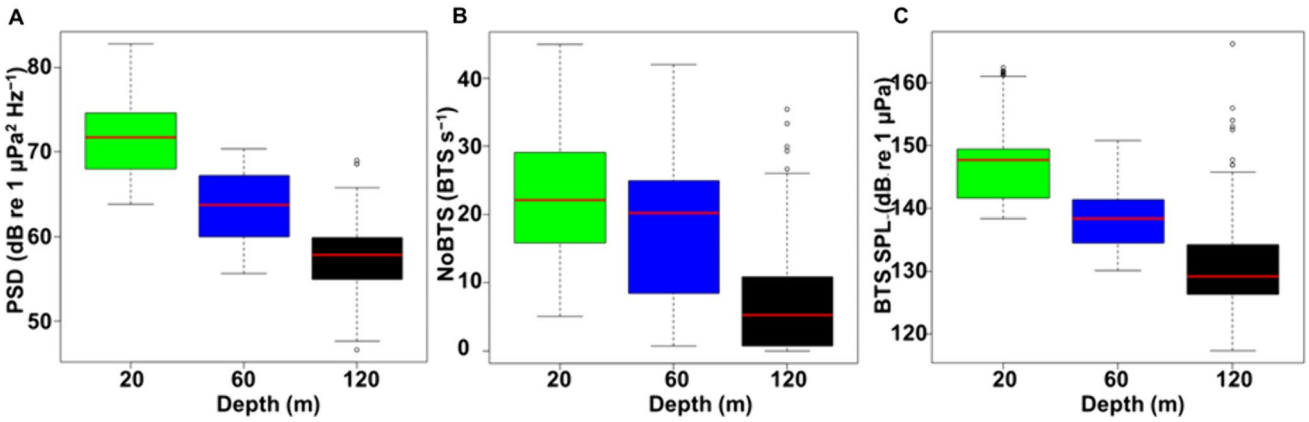

Fig. 4 Depth variation of acoustic features: **A** PSD_{Fpeak} highest power spectral density value. **B** NoBTS number of broadband transient sounds, and **C** BTS SPL_{pp} peak-to-peak sound pressure level of the broadband transient sounds. In green: 20 m, in blue: 60 m and in black: 120 m. Whiskers represent 1.5 inter-quartile range. Data falling outside the Q1–Q3 range are plotted as outliers of the data

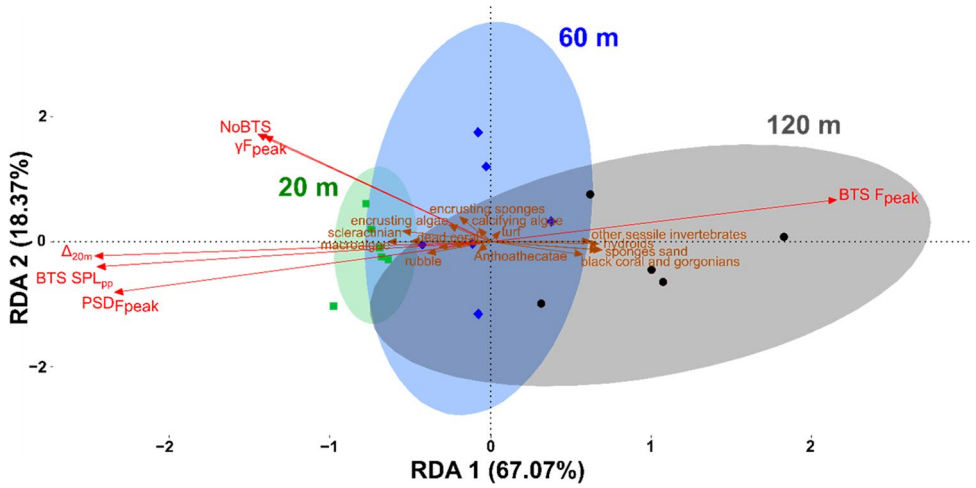

Fig. 5 Redundancy analysis (RDA) plot examining the link between benthic cover features and acoustic features. Ellipses are 95% confidence interval. Red arrows indicate acoustic features while brown arrows indicate benthic cover features. In green: 20 m, in blue: 60 m, and in black: 120 m. PSD_{Fpeak} highest power spectral density value, γFpeak corresponding frequency, Δ20m difference between the peak frequency at 20 m compared to the corresponding frequency at 60 or 120 m, BTS SPL_{pp} peak-to-peak sound pressure level of the broadband transient sounds, NoBTS number of broadband transient sounds, and BTS Fpeak peak frequency of the broadband transient sounds

invertebrates varied along the depth gradient, ranging from altiphotic reefs to the upper part of mesophotic reefs, and notably in the lower part of mesophotic reefs. These depth-related differences may be associated with a decrease in temperature (Watanabe et al. 2002), an increase in the distance from shore (Di Iorio et al. 2021), or the transition from a light-dependent scleractinian-dominated reef with macroalgae to a sandy reef with a higher number of sponges, black corals, and gorgonians (Butler et al. 2017). However, not all measured acoustic features showed linear trends. For sound-pressure level and power spectral density (SPL_{pp} and PSD_{Fpeak}), the greater the depth, the lower the sound-pressure levels, with an average decrease of 6–8 dB re 1 μPa^2Hz^{-1} at 60 m compared to 20 m, and at 120 m compared to 60 m. In contrast, regarding the number of BTS, the number of nocturnal BTSs was generally higher at 60 m than at 20 m. This might seem counter-intuitive, as a higher number of sounds would typically be associated with higher sound-pressure levels. "Intensity features" (i.e., PSD and BTS SPL_{pp}) and NoBTS may thus provide different information related to biodiversity or invertebrate communities. Higher coral diversity at the level of genus in French Polynesia has been reported at 60 m compared to 20 m depth (Pérez-Rosales et al. 2022a), which could consequently explain a higher diversity of sessile benthic invertebrate fauna and the increased BTS observed at 60 m depth. There are also alternative explanations. On one hand, the upper part of the mesophotic reefs (60 m) could shelter more sound-emitting specimens or species producing more sounds than in altiphotic reefs. On the other hand, altiphotic reefs seem to shelter species producing louder sounds than in the upper part of the mesophotic reefs, as indicated by the highest levels of SPL_{pp} and $PSD_{Fpeak.}$ Altiphotic reefs are dominated by snapping shrimp sounds, which are among the loudest marine sounds emitted by benthic invertebrates (Au and Banks 1998). Therefore, even in smaller numbers, they could be responsible for the observed increase in sound levels at 20 m depth. Alternatively, snapping shrimp sounds create mass phenomena that elevate ambient noise levels, potentially reducing the signal-to-noise ratio and thus negatively biasing the outcomes of the automatic detector in the altiphotic zone.

Unlike the reefs at 20–60 m, the deeper part of the mesophotic reef (120 m) exhibited considerably lower acoustic activity. This finding aligns with Everest et al. (1948), who reported that beyond a depth of 55 m, and regardless of environmental suitability (Johnson et al. 1947), the noise levels of snapping shrimp sounds decrease. Below 61–91 m, the presence of snapping shrimp noise is unlikely, unless transmitted from nearby shallower areas (UCDWR 1946). The absence of snapping shrimp sounds may therefore account for the absence of the continuous crackle typically found in shallow habitats (Johnson et al. 1947). The lower concentration of deep living species (UCDWR 1946; Johnson et al. 1947; Hurley et al. 2016; Anker 2020) also likely contributes to the reduction of BTS recorded at 120 m depth. It has been hypothesized that the increased number of invertivores in the mesophotic reefs may explain the decrease in crustacean sound intensity with depth observed in Japanese reefs (Lin et al. 2021). The reduction of canopy-forming algae has also been suggested as a potential cause for the decrease in

Table 3 Mean percentage of benthic cover per island and per depth (N = 30 per depth per island)

	Sand	Non encrusting sponges	Turf	Consolidated substrate	Black coral and gorgonians	Calcifying algae	Anthoathecata	Encrusting sponges	Other sessile invertebrates	Rubble	Other hydroids	Scleractinian	Macroalgae including *Halimeda*	Dead coral	Fleshy algae	Encrusting algae
Bora Bora																
20 m	9	1.2	0	30.3	0	0.5	0	0.2	0	22.4	0	35.1	1	0.4	0	0
60 m	0.6	5.5	0	16.8	0	6	0.3	1.6	0	0.1	0	68.3	0.5	0	0	0
120 m	42.3	12.8	6.2	19.4	7.1	4.4	0	0.4	0	5.6	0.6	1.2	0	0	0	0.1
Mangareva																
20 m	0.8	0	0	39.8	0	8.2	0.5	0	0	1	0	43.6	3.1	2.7	0	0.4
60 m	18.1	0.1	5.6	22.3	0	2.5	0	0.1	0	1.6	0	9.4	1.2	1.9	0	36.9
Moorea																
20 m	7.8	0.4	0	32.9	0	6.4	0	0.5	0	10.3	0	38	3.3	0.1	0	0
60 m	23.4	0.7	0	45.4	0	14	0	0	0	0.7	0	15.3	0	0	0	0.4
120 m	29.6	21.9	11	22.1	2.9	3.3	0	0	2.9	2.9	2.8	0.3	0	0	0	0
Rangiroa																
20 m	4	1	0	35.1	0	3.8	0	2	0	23	0	11.1	0.6	0.1	0	19.2
60 m	42	8.6	4.1	15.8	0	1.1	0	4.2	0	1.9	0	22	0	0	0	0.2
120 m	50.1	21.9	12.5	12.5	0.2	0.5	0.3	0.3	0.2	0.1	0.1	0	0	0	0	0
Raroia																
20 m	0	0	0	19.1	0	8.7	0	9.6	0	0	0	56.1	1.8	4.6	0	0
60 m	16.9	0.5	0	44.1	0	4.2	0	11	0	4.7	0	18.5	0	0	0	0
120 m	57.9	8.7	0	20.8	0	10.7	0	0.9	0	0.6	0	0.3	0	0	0	0
Tikehau																
20 m	2.2	5.1	28.1	11.2	0	6.1	0	0	0.2	7.6	0	32.1	1.9	3.3	0.6	1.2
60 m	28.9	6.3	12.8	3.8	0	11.2	0	0	0.1	3.6	0	32.4	0	0.1	0.1	0.4
120 m	79.8	1.8	0	9.2	0.1	3.4	0	0	0.2	5.2	0	0	0	0	0	0

Table 4 Linear mixed-effect model (per depth) results with multiple comparisons (Tukey tests) to access diel variability

Feature	Comparison	20 m		60 m		120 m	
		Z value	*P*	Z value	*P*	Z value	*P*
PSD_{Fpeak}		F = 18.58, ***P* < .0001**, N = 66		F = 19.84, ***P* < .0001**, N = 66		F = 1.63, *P* = 0.19, N = 55	
	Night–day	7.00	**< .0001**	7.05	**< .0001**		
	SR – day	3.36	**0.0047**	2.86	**0.026**		
	SS – day	5.64	**< .0001**	5.65	**< .0001**		
	SR – night	− 4.07	**0.00028**	− 4.69	**< .0001**		
	SS – night	− 1.52	0.78	− 1.56	0.71		
	SS – SR	2.55	0.064	3.13	**0.011**		
γFpeak		F = 2.82, ***P* = 0.0465**, N = 66		F = 1.96, *P* = 0.13, N = 66		F = 1.87, *P* = 0.15, N = 55	
	Night – day	− 1.97	0.29				
	SR – day	− 0.030	≈ 1.00				
	SS – day	− 1.92	0.33				
	SR – night	2.17	0.18				
	SS – night	0.049	≈ 1.00				
	SS – SR	− 2.12	0.20				
Δ_{20}				F = 0.12, *P* = 0.95, N = 66		F = 1.26, *P* = 0.30, N = 55	
BTS SPL_{pp}		F = 608.98, ***P* < .0001**, N = 2152		F = 987.58, ***P* < .0001** N = 2028		F = 106.73, ***P* < .0001**, N = 1552	
	Night – day	42.34	**< .0001**	53.60	**< .0001**	17.20	**< .0001**
	SR – day	13.39	**< .0001**	16.67	**< .0001**	3.80	**0.00086**
	SS – day	20.62	**< .0001**	28.13	**< .0001**	9.87	**< .0001**
	SR – night	− 14.08	**< .0001**	− 19.44	**< .0001**	− 7.57	**< .0001**
	SS – night	− 6.55	**< .0001**	− 7.22	**< .0001**	− 1.24	≈ 1.00
	SS – SR	5.86	**< .0001**	9.50	**< .0001**	4.94	**< .0001**
NoBTS		F = 52.37, ***P* < .0001**, N = 2152		F = 69.20, ***P* < .0001** N = 2028		F = 7.41, ***P* = 0.0001**, N = 1552	
	Night – day	12.46	**< .0001**	− 14.24	**< .0001**	4.31	**< .0001**
	SR – day	− 3.77	**0.00099**	− 4.02	**0.00035**	3.06	**0.013**
	SS – day	− 5.35	**< .0001**	− 5.30	**< .0001**	3.00	**0.016**
	SR – night	4.32	**< .0001**	5.60	**< .0001**	0.33	≈ 1.00
	SS – night	2.68	**0.044**	4.23	**0.00014**	0.23	≈ 1.00
	SS – SR	− 1.28	≈ 1.00	− 1.06	≈ 1.00	− 0.082	≈ 1.00
BTS Fpeak		F = 4.52, ***P* = 0.0036**, N = 2130		F = 23.26, ***P* < .0001** N = 1994		F = 6.89, **P = 0.0001**, N = 1341	
	Night – day	− 1.25	≈ 1.00	− 8.28	**< .0001**	− 4.44	**< .0001**
	SR – day	− 14.47	0.85	− 3.18	**0.0087**	− 0.92	≈ 1.00
	SS – day	− 3.61	**0.0018**	− 4.38	**< .0001**	− 2.04	0.25
	SR – night	− 0.72	≈ 1.00	2.35	0.11	1.97	0.29
	SS – night	− 2.98	**0.018**	1.02	≈ 1.00	0.80	≈ 1.00
	SS – SR	− 1.75	0.48	1.02	≈ 1.00	− 0.91	≈ 1.00

P-values are adjusted with Bonferroni corrections. **PSD_{Fpeak}** = highest power spectral density value, **γFpeak** = corresponding frequency, **Δ20m** = difference between the peak frequency at 20 m compared to the corresponding frequency at 60 or 120 m, **BTS SPL_{pp}** = peak-to-peak sound pressure level of the broadband transient sounds, **NoBTS** = number of broadband transient sounds, and **BTS Fpeak** = peak frequency of the broadband transient sounds. α = 0.05, SR = sunrise, SS = sunset

snapping shrimp sound production, favouring opportunistic turf-forming algae (Connell et al. 2013; Rossi et al. 2016; Nagelkerken et al. 2016).

Acoustic variables also differed among islands. For instance, in Moorea, the most significant decrease in PSD_{Fpeak} occured between 60 and 120 m. At a depth of

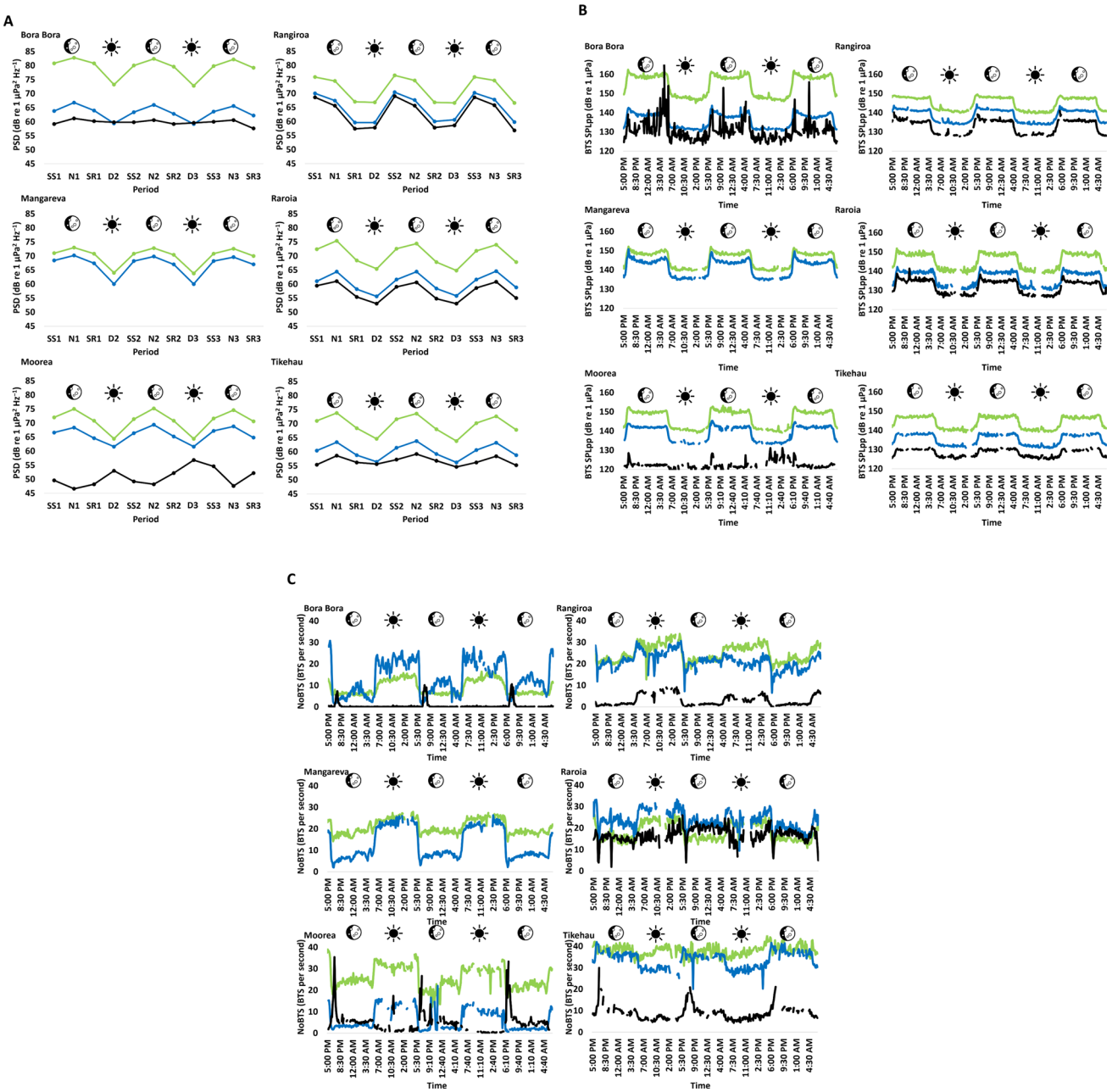

Fig. 6 Diel pattern of the BTS. **A** The highest power spectral density value (PSDFpeak), **B** peak-to-peak sound pressure level of the broadband transient sounds (BTS SPL_{pp}), and **C** number of broadband transient sounds (NoBTS). Depths are indicated as following: green 20 m, blue 60 m, and black 120 m. Sun and moon symbols indicate day and night periods respectively. For panel **A**, periods are used (SS = sunset, N = night, SR = sunrise, and D = day) while time series are showed for panels **B** and **C**

120 m, Moorea diverged from other islands due to higher percentages of black coral (1.3% vs. 0 to 0.09%), hydroids (2.8% vs. 0 to 0.6%) and sessile invertebrates (2.9% vs. 0 to 0.18%), as well as a lower temperature. Temperature has been reported as positively correlated with the number of snap sounds (Watanabe et al. 2002; Lillis and Mooney 2018). Previous studies have demonstrated that differences in bottom types can influence sounds. At equivalent depths, less intense sounds have been observed from non-favourable bottom types compared to favorable ones for snapping-shrimps (e.g., coral, rock, stone, and shell) (UCDWR 1946). Additionally, at Rangiroa; PSD_{Fpeak} values at 20 m were significantly higher than in the other islands. This might be explained by the unique geomorphological features of the site (Everest et al. 1948). However, further investigation is necessary for a comprehensive understanding.

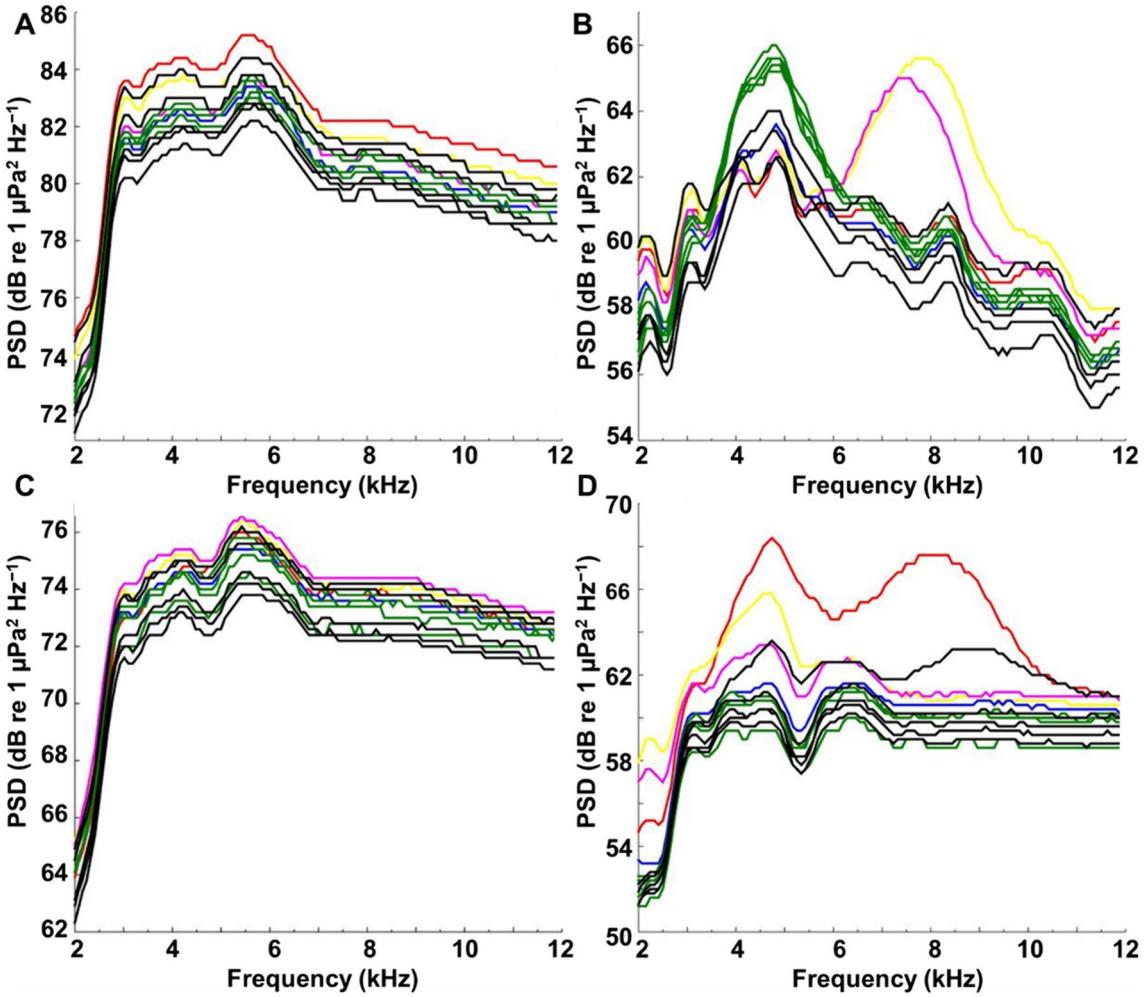

Fig. 7 Examples of the detailed variation of Power Spectral density (PSD) between 6:20 PM and 8:30 PM for two islands (Bora Bora and Raroia). Graphs are median PSD between 2 and 12 kHz. **A** Bora Bora 20 m**, B** Bora Bora 120 m, **C** Raroia 20 m, **D** Raroia 120 m. Red: 6:30 PM, yellow: 6:40 PM, magenta: 6:50 PM, blue: 7 PM, green: 7:10 to 7:40 PM, black: 7:50 to 8:30 PM

The differences observed in spectral frequencies (γFpeak) suggest the presence of distinct mass phenomena. However, a consistent trend specific to depth was not identified. These variations may be associated with differences in associated crustaceans communities, given that peak frequencies vary depending on the emitting species (Hazlett and Winn 1962a; Knowlton and Moulton 1963; Readhead 1997; Au and Banks 1998). They could also result from differences in the abundances of species present with sounds of varying peak frequencies. Alternatively, single BTS can have multiple frequency peaks (Everest et al. 1948; Coquereau et al. 2016) leading to distinct spectral increases. The broadband nature of snapping shrimp sounds complicates the association between specific species and the identification of recorded peak frequencies.

In reefs, high-frequency sounds other than those of snapping shrimp, which predominantly fall within the 2–20 kHz range (UCDWR 1946), can also be recorded. For instance, interactions between hard-shelled benthic macro-organisms and the coral substrate contribute to a peak between 11 and 17 kHz, centred at 14.3 and 14.6 kHz (Freeman et al. 2014). Higher frequencies can be emitted by certain species of Palinuridae (Buscaino et al. 2011). Conversely, lower frequencies are known to be produced by some species of Palinuridae (Moulton 1957; Hazlett and Winn 1962b; Mulligan and Fischer 1977; Patek et al. 2009) and Penaeidae (Berk 1997; Silva et al. 2019; Wei et al. 2020). In temperate areas, bivalves are known to produce high frequency sounds (Di Iorio et al. 2012), while sea urchins are known to emit lower-frequency sounds (between 0.7 and 2.8 kHz) with relatively lower peak frequencies during feeding (Radford et al. 2008). However, in Polynesian reefs, this frequency range does not correspond to a spectral increase (Raick et al. 2021).

Diel variability

Overall, benthic activity rhythms at 120 m exhibited low or highly variable levels of diel variation, likely due to reduced solar irradiation. Between-island variability was most pronounced at 120 m. Notably, distinctive rhythmic patterns were observed in terms of number of BTS. One particular observation in the soundscapes at 120 m in Bora Bora, Moorea, and Tikehau was a daily peak in the number of BTS around 5.4 kHz, consistently occurring at 7 PM. Since the sounds forming the peak shared the same peak frequency, it is likely that these peaks represent cyclic activity of a specific species. To our knowledge, this sound has not been previously described, and its peak frequency does not match descriptions of animals in mesophotic reefs. Moreover, its presence on different islands from different archipelagos and during various nights indicates it is not anecdotical but reflects a cyclic biological activity of a particular species or deep-adapted ecological groups. At 20–60 m depths, benthic activity rhythms were more similar compared to those at 120 m depth. They also exhibited pronounced diel variations with higher PSD and BTS SPL_{pp} during the night. This aligns with studies in the Caribbeans (Lillis and Mooney 2016) and Polynesia (Raick et al. 2021). The number of BTS showed opposite trends, with higher values during the day. In Moorea, recordings made at 12 m revealed that the number of BTS could vary differently between day and night depending on the frequency band (Raick et al. 2021). During the night, the number of BTS in the 3.5 – 5.5 kHz band was 8% higher, while in higher frequency bands (6 – 8 kHz and 10 – 13 kHz), it was 14% to 5% lower compared to the day (Raick et al. 2021).

Conclusion

This study identifies for the first time acoustic patterns from altiphotic to mesophotic coral reefs associated with the activity of benthic invertebrates. The observed differences can reflect community composition or different behaviors. The findings emphasize the marked differences in the deeper part of the mesophotic reefs compared to the upper part at 60 m depth and the altiphotic zone, likely indicative of variations in biodiversity or community composition linked to benthic sessile cover features such as hydroids, sponges, black corals and gorgonians. These features can create animal forests, three-dimensional structures hosting a variety of small cryptic organisms (Rossi et al. 2017; Poupin et al. 2022). Furthermore, the limited occurrence of diel patterns at 120 m suggests that reduced light regimes influence biorhythms. Studies linking habitat variables to acoustics are still scarce but necessary to understand habitat-specific patterns and the drivers of acoustic variations (Di Iorio et al. 2021; Raick et al. 2023). The results presented here support the use of passive acoustics for the study and monitoring of mesophotic reefs. In these challenging-to-access environments, where species are often cryptic, ecoacoustic approaches offer unprecedented opportunities for assessing the spatio-temporal dynamics of mesophotic reefs.

Supplementary Information The online version contains supplementary material available at https://doi.org/10.1007/s00442-024-05572-5.

Acknowledgements We thank the diving team from Under The Pole and the crew of UTP III Expedition for their help during sampling in French Polynesia. We thank Laetitia Hédouin for her help with funding acquisition.

Under the Pole Expeditions, 1 Rue des Senneurs, Concarneau, France. Members: G. Bardout, J. Fauchet, A. Ferucci, F. Gazzola, G. Lagarrigue, J. Leblond, E. Marivint, A. Mittau, N. Mollon, N. Paulme, E. Périé-Bardout, R. Pete, S. Pujolle, G. Siu.

Author contribution statement XR analyzed and interpreted the acoustic data under the supervision of LDI. XR wrote the first version of the manuscript. XR, LDI and EP wrote the final version of the manuscript with inputs from FB, GPR, and HR. LDI and XR conceived the analyzes. DL helped with funding acquisition. CG provided algorithms. UTP dove to place the acoustic equipment and photography photoquadrats. GPR and HR provided data from cover quadrats analyses and coordinated the deployment of the acoustic equipment. FB prepared the acoustic equipment for the sampling and stored the data.

Funding This research was funded by the ANR DEEPHOPE (ANRAAPG 2017 #168722), the Délégation à la Recherche DEEPCORAL, the CNRS DEEPREEF and the IFRECOR. The technical dives were funded through the Under The Pole Expedition III.

Data availability The data that support the findings of this study are available on request from the corresponding author (XR) and/or within the supplementary materials.

Declarations

Conflict of interest All authors declare that they have no conflicts of interest.

References

Anker A (2020) On two new deep-water snapping shrimps from the Indo-West Pacific (Decapoda: Alpheidae: Alpheus). Zootaxa 4845:393–409. https://doi.org/10.11646/zootaxa.4845.3.5

Au WWL, Banks K (1998) The acoustics of the snapping shrimp *Synalpheus parneomeris* in Kaneohe Bay. J Acoust Soc Am Doi. https://doi.org/10.1121/1.423234

Baldwin CC, Tornabene L, Robertson DR (2018) Below the Mesophotic. Sci Rep 8:4920. https://doi.org/10.1038/s41598-018-23067-1

Berk IM (1997) Sound production by white shrimp (Penaeus setiferus) analysis of another crustacean-like sound from the Gulf of Mexico, and the possible use of passive sonar for dedication and stock assessment of shrimp. Master's thesis, Texas A&M University. Available electronically from https://hdl.handle.net/1969.1/ETD-TAMU-1997-THESIS-B46

Bertucci F, Parmentier E, Lecellier G et al (2016) Acoustic indices provide information on the status of coral reefs: An example from

Moorea island in the south pacific. Sci Rep 6:1–9. https://doi.org/10.1038/srep33326
Bertucci F, Maratrat K, Berthe C et al (2020) Local sonic activity reveals potential partitioning in a coral reef fish community. Oecologia. https://doi.org/10.1007/s00442-020-04647-3
Bolgan M, Gervaise C, Di Iorio L et al (2020) Fish biophony in a mediterranean submarine canyon. J Acoust Soc Am 147:2466–2477. https://doi.org/10.1121/10.0001101
Buscaino G, Filiciotto F, Gristina M et al (2011) Acoustic behaviour of the European spiny lobster Palinurus elephas. Mar Ecol Prog Ser 441:177–184. https://doi.org/10.3354/meps09404
Butler J, Butler MJ, Gaff H (2017) Snap, crackle, and pop: acoustic-based model estimation of snapping shrimp populations in healthy and degraded hard-bottom habitats. Ecol Indic 77:377–385. https://doi.org/10.1016/j.ecolind.2017.02.041
Chin Y-Y, Prince J, Kendrick G, Abdul Wahab MA (2020) Sponges in shallow tropical and temperate reefs are important habitats for marine invertebrate biodiversity. Mar Biol 167:164. https://doi.org/10.1007/s00227-020-03771-1
Connell SD, Kroeker KJ, Fabricius KE et al (2013) The other ocean acidification problem: CO2 as a resource among competitors for ecosystem dominance. Philos Trans R Soc B Biol Sci 368:20120442. https://doi.org/10.1098/rstb.2012.0442
Coquereau L, Grall J, Chauvaud L et al (2016) Sound production and associated behaviours of benthic invertebrates from a coastal habitat in the north-east Atlantic. Mar Biol 163:127. https://doi.org/10.1007/s00227-016-2902-2
Desjonquères C, Rybak F, Castella E et al (2018) Acoustic communities reflects lateral hydrological connectivity in riverine floodplain similarly to macroinvertebrate communities. Sci Rep 8:14387. https://doi.org/10.1038/s41598-018-31798-4
Di Iorio L, Gervaise C, Jaud V et al (2012) Hydrophone detects cracking sounds: Non-intrusive monitoring of bivalve movement. J Exp Mar Bio Ecol 432–433:9–16. https://doi.org/10.1016/j.jembe.2012.07.010
Di Iorio L, Audax M, Deter J et al (2021) Biogeography of acoustic biodiversity of NW mediterranean coralligenous reefs. Sci Rep 11:16991. https://doi.org/10.1038/s41598-021-96378-5
Díaz MC, Rützler K (2001) Sponges: An essential component of caribbean coral reefs. Bull Mar Sci 69:535–546
Everest FA, Young RW, Johnson MW (1948) Acoustical characteristics of noise produced by snapping shrimp. J Acoust Soc Am 20:137–142
Favaro L, Cresta E, Friard O et al (2021) Passive acoustic monitoring of the endangered African Penguin (*Spheniscus demersus*) using autonomous recording units and ecoacoustic indices. Ibis 163:1472–1480. https://doi.org/10.1111/ibi.12970
Ferguson BG, Cleary JL (2001) In situ source level and source position estimates of biological transient signals produced by snapping shrimp in an underwater environment. J Acoust Soc Am 109:3031–3037. https://doi.org/10.1121/1.1339823
Freeman SE, Rohwer FL, D'Spain GL et al (2014) The origins of ambient biological sound from coral reef ecosystems in the Line Islands archipelago. J Acoust Soc Am 135:1775–1788. https://doi.org/10.1121/1.4865922
Gervaise C, Lossent J, Valentini-Poirier CA et al (2019) Three-dimensional mapping of the benthic invertebrates biophony with a compact four-hydrophones array. Appl Acoust. https://doi.org/10.1016/j.apacoust.2018.12.025
Gibb R, Browning E, Glover-Kapfer P, Jones KE (2019) Emerging opportunities and challenges for passive acoustics in ecological assessment and monitoring. Methods Ecol Evol 10:169–185. https://doi.org/10.1111/2041-210X.13101
Goreau T, Goreau N (1973) The ecology of Jamaican coral reefs. II. geomorphology, zonation, and sedimentary phases. Bull Mar Sci 23:399–464
Hazlett B, Winn HE (1962a) Sound producing mechanism of the nassau grouper *Epinephelus striatus*. Copeia 2:447–449
Hazlett BA, Winn HE (1962b) Characteristics of a sound produced by the lobster *Justitia longimanus*. Ecology 43:741–742. https://doi.org/10.2307/1933469
Hinderstein LM, Marr JCA, Martinez FA et al (2010) Mesophotic coral ecosystems: characterization, ecology, and management. Coral Reefs 29:247–251. https://doi.org/10.1007/s00338-010-0614-5
Hurley KKC, Timmers MA, Godwin LS et al (2016) An assessment of shallow and mesophotic reef brachyuran crab assemblages on the south shore of O'ahu, Hawai'i. Coral Reefs 35:103–112. https://doi.org/10.1007/s00338-015-1382-z
Jézéquel Y, Bonnel J, Coston-Guarini J et al (2018) Sound characterization of the European lobster *Homarus gammarus* in tanks. Aquat Biol 27:13–23. https://doi.org/10.3354/ab00692
Johnson MW, Everest FA, Young RW (1947) The role of snapping shrimp (*Crangon* and *Synalpheus*) in the production of underwater noise in the sea. Biol Bull 93:122–138. https://doi.org/10.2307/1538284
Johnson MW (1944) Underwater noise and the distribution of snapping shrimp with special reference to the asiatic and the southwest and central Pacific areas. Library – Scripps Digital Collection, UC San Diego. Retrieved from https://escholarship.org/uc/item/90s6t2x1
Kahng SE, Kelley CD (2007) Vertical zonation of megabenthic taxa on a deep photosynthetic reef (50–140 m) in the Au'au channel. Hawaii Coral Reefs 26:679–687. https://doi.org/10.1007/s00338-007-0253-7
Kennedy EV, Holderied MW, Mair JM et al (2010) Spatial patterns in reef-generated noise relate to habitats and communities: evidence from a panamanian case study. J Exp Mar Biol Ecol 395:85–92. https://doi.org/10.1016/j.jembe.2010.08.017
Knowlton RE, Moulton JM (1963) Sound production in the snapping shrimps *Alpheus* (*Crangon*) and *Synalpheus*. Biol Bull 125:311–331. https://doi.org/10.2307/1539406
Kopp D, Bouchon-Navaro Y, Louis M et al (2012) Spatial and temporal variation in a caribbean herbivorous fish assemblage. J Coast Res 278:63–72. https://doi.org/10.2112/JCOASTRES-D-09-00165.1
Ladich F (2015) Communication in fishes. Sound communication in fishes. Springer, Vienna, pp 127–148
Lammers MO, Brainard RE, Au WWL et al (2008) An ecological acoustic recorder (EAR) for long-term monitoring of biological and anthropogenic sounds on coral reefs and other marine habitats. J Acoust Soc Am 123:1720–1728. https://doi.org/10.1121/1.2836780
Lesser M, Slattery M, Leichter J (2009) Ecology of mesophotic coral reefs. J Exp Mar Bio Ecol 375:1–8
Lesser MP, Slattery M, Laverick JH et al (2019) Global community breaks at 60 m on mesophotic coral reefs. Glob Ecol Biogeogr 28:1403–1416. https://doi.org/10.1111/geb.12940
Liddell WD, Ohlhorst SL (1988) Hard substrata community patterns, 1–120 M. North Jamaica Palaios 3:413. https://doi.org/10.2307/3514787
Lillis A, Mooney TA (2016) Loudly heard, little seen, and rarely understood: spatiotemporal variation and environmental drivers of sound production by snapping shrimp. Proc Meet Acoust. https://doi.org/10.1121/2.0000270
Lillis A, Mooney TA (2018) Snapping shrimp sound production patterns on Caribbean coral reefs: relationships with celestial cycles and environmental variables. Coral Reefs 37:597–607. https://doi.org/10.1007/s00338-018-1684-z
Lin T-H, Chen C, Watanabe HK et al (2019) Using soundscapes to assess deep-sea benthic ecosystems. Trends Ecol Evol 34:1066–1069. https://doi.org/10.1016/j.tree.2019.09.006
Lin T-H, Akamatsu T, Sinniger F, Harii S (2021) Exploring coral reef biodiversity via underwater soundscapes. Biol Conserv 253:108901. https://doi.org/10.1016/j.biocon.2020.108901

Loya Y, Puglise KA, Bridge TCL (2019) Mesophotic Coral Ecosystems. Springer International Publishing, Cham

Milligan RJ, Spence G, Roberts JM, Bailey DM (2016) Fish communities associated with cold-water corals vary with depth and substratum type. Deep Sea Res Part I Oceanogr Res Pap 114:43–54. https://doi.org/10.1016/j.dsr.2016.04.011

Minier L, Bertucci F, Raick X et al (2023a) Characterization of the different sound sources within the soundscape of coastline reef habitats (Bora Bora, French Polynesia). Estuar Coast Shelf Sci 294:108551. https://doi.org/10.1016/j.ecss.2023.108551

Minier L, Raick X, Gairin E et al (2023b) 'Habitat-associated soundscape' hypothesis tested on several coral reefs within a lagoon (Bora-Bora Island, French Polynesia). Mar Biol 170:61. https://doi.org/10.1007/s00227-023-04206-3

Mooney TA, Di Iorio L, Lammers M et al (2020) Listening forward: approaching marine biodiversity assessments using acoustic methods: acoustic diversity and biodiversity. R Soc Open Sci 7:201287. https://doi.org/10.1098/rsos.201287

Moulton JM (1957) Sound production in the spiny lobster *Panulirus argus* (Latreille). Biol Bull 113:286–295

Mulligan BE, Fischer RB (1977) Sounds and behavior of the spiny lobster *Panulirus argus* (Latreille, 1804) (Decapoda, Palinuridae). Crustaceana 32:185–199

Nagelkerken I, Russell BD, Gillanders BM, Connell SD (2016) Ocean acidification alters fish populations indirectly through habitat modification. Nat Clim Chang 6:89–93. https://doi.org/10.1038/nclimate2757

Oksanen J, Blanchet FG, Kindt R, Legendre P, Minchin PR, O'Hara RB, Simpson GL, Solymos P, Stevenes MHH, Wagner H (2012) Vegan: community ecology package. R package version 2.0–2

Patek SN, Shipp LE, Staaterman ER (2009) The acoustics and acoustic behavior of the California spiny lobster (*Panulirus interruptus*). J Acoust Soc Am 125:3434. https://doi.org/10.1121/1.3097760

Pérez-Rosales G, Hernández-Agreda A, Bongaerts P et al (2022a) Mesophotic depths hide high coral cover communities in French Polynesia. Sci Total Environ 844:157049. https://doi.org/10.1016/j.scitotenv.2022.157049

Pérez-Rosales G, Pichon M, Rouzé H, Villéger S, Torda G, Bongaerts P, Carlot J, Parravicini V, Hédouin L (2022b) Mesophotic coral ecosystems of French Polynesia are hotspots of alpha and beta generic diversity for scleractinian assemblages. Divers Distrib. https://doi.org/10.1111/ddi.13549

Piercy JJB, Codling EA, Hill AJ et al (2014) Habitat quality affects sound production and likely distance of detection on coral reefs. Mar Ecol Prog Ser 516:35–47. https://doi.org/10.3354/meps10986

Pijanowski BC, Farina A, Gage SH et al (2011) What is soundscape ecology? An introduction and overview of an emerging new science. Landsc Ecol 26:1213–1232. https://doi.org/10.1007/s10980-011-9600-8

Poupin J, Barathieu G, Konieczny O, Mulochau T (2022) Crustacés (Decapoda Stomatopoda) dans la zone mésophotique corallienne de Mayotte (Sud-Ouest Océan Indien). Naturae. https://doi.org/10.5852/naturae2022a8

Pyle RL, Boland R, Bolick H et al (2016) A comprehensive investigation of mesophotic coral ecosystems in the Hawaiian Archipelago. PeerJ 2016:1–45. https://doi.org/10.7717/peerj.2475

Pyle RL, Copus JM (2019) Mesophotic coral ecosystems: introduction and overview. In: Loya Y, Puglise K, Bridge T (eds) Mesophotic coral ecosystems. Coral reefs of the world, vol 12. Springer, Cham. https://doi.org/10.1007/978-3-319-92735-0_1

Radford C, Jeffs A, Tindle C, Montgomery JC (2008) Resonating sea urchin skeletons create coastal choruses. Mar Ecol Prog Ser 362:37–43. https://doi.org/10.3354/meps07444

Radford CA, Stanley JA, Hole W et al (2010) Localised coastal habitats have distinct underwater sound signatures. Mar Ecol Prog Ser 401:21–29. https://doi.org/10.3354/meps08451

Radford CA, Stanley JA, Jeffs AG (2014) Adjacent coral reef habitats produce different underwater sound signatures. Mar Ecol Prog Ser 505:19–28. https://doi.org/10.3354/meps10782

Raick X, Di Iorio L, Gervaise C et al (2021) From the reef to the ocean: revealing the acoustic range of the biophony of a coral reef (Moorea Island, French Polynesia). J Mar Sci Eng 9:420. https://doi.org/10.3390/jmse9040420

Raick X, Di Iorio L, Lecchini D et al (2023a) Fish sounds of photic and mesophotic coral reefs: variation with depth and type of island. Coral Reefs. https://doi.org/10.1007/s00338-022-02343-7

Raick X, Collet P, Under The Pole Consortium, Lecchini D, Bertucci F, Parmentier E (2023b) Diel cycle of two recurrent fish sounds from mesophotic coral reefs. Scientia Marina 87(4):078. https://doi.org/10.3989/scimar.05395.078.

Ramette A (2007) Multivariate analyses in microbial ecology. FEMS Microbiol Ecol 62:142–160. https://doi.org/10.1111/j.1574-6941.2007.00375.x

Rancher J, Rougerie F (1994) L'environnement océanique de l'archipel des Tuamotu (Polynésie Française). Oceanol Acta- 18:43–60

Rao CR (1964) The use and interpretation of principal component analysis in applied research. Sankhyā Indian J Stat Ser A 26:329–358

Readhead ML (1997) Snapping shrimp noise near gladstone, Queensland. J Acoust Soc Am 101:1718–1722. https://doi.org/10.1121/1.418153

Rossi T, Connell SD, Nagelkerken I (2016) Silent oceans: ocean acidification impoverishes natural soundscapes by altering sound production of the world's noisiest marine invertebrate. Proc R Soc B Biol Sci. https://doi.org/10.1098/rspb.2015.3046

Rossi S, Bramanti L, Gori A, Orejas C (2017) An overview of the animal forests of the world. Marine Animal Forests. Springer International Publishing, Cham, pp 1–26

Rougerie F, Fichez R, Déjardin P (1997) Geomorphology and hydrogeology of selected islands of French Polynesia: Tikeahau (atoll) and Tahiti (barrier reef). Geology and Hydrogeology of Carbonate Islands. Developments in Sedimentology, Elsevier, NY

Silva JF, Hamilton S, Rocha JV et al (2019) Acoustic characterization of feeding activity of *Litopenaeus vannamei* in captivity. Aquaculture 501:76–81. https://doi.org/10.1016/j.aquaculture.2018.11.013

Sueur J, Farina A (2015) Ecoacoustics: the ecological investigation and interpretation of environmental sound. Biosemiotics 8:493–502. https://doi.org/10.1007/s12304-015-9248-x

ter Braak CJF (1994) Canonical community ordination. Part I: basic theory and linear methods. Écoscience 1:127–140. https://doi.org/10.1080/11956860.1994.11682237

UCDWR (1946) Underwater noise caused by snapping shrimp. University of California, Division of war research, The U.S. Navy Electronics Laboratory Contract Nobs - 2074 Navy Department, Bureau of Ships 2G, UCDWR No U337 file No 01.331, 1 April 1946

Watanabe M, Sekine M, Hamada E et al (2002) Monitoring of shallow sea environment by using snapping shrimps. Water Sci Technol 46:419–424. https://doi.org/10.2166/wst.2002.0772

Wei M, Lin Y, Chen K et al (2020) Study on feeding activity of *Litopenaeus vannamei* based on passive acoustic detection. IEEE Access 8:156654–156662. https://doi.org/10.1109/ACCESS.2020.3019529

Weinstein DK, Klaus JS, Smith TB (2015) Habitat heterogeneity reflected in mesophotic reef sediments. Sediment Geol 329:177–187. https://doi.org/10.1016/j.sedgeo.2015.07.003